

Specific heat and thermal conductivity of dielectrics at low temperatures

M. D. Tiwari*

*Institut für Angewandte Physik, Universität Münster, D-4400 Münster,
Federal Republic of Germany*

(Received 13 May 1981)

Relaxation time of lattice waves for a nonideal lattice has been obtained by using the T -matrix Green's-function method. The T matrix for a defect which affects both the mass and the short-range interaction is taken into consideration for analyzing the irreducible representations of the point group pertaining to the perturbation. The resonances from F_{1u} , A_{1g} , and E_g symmetry modes are discussed in detail for anion as well as cation impurities (Tl^+ , Br^- , I^- , Cs^+ , Na^+ , and Ag^+) in KCl crystals. A breathing-shell model with second-neighbor interactions is employed for a description of the host-lattice dynamics. Maxima are observed in the relative variation of $\Delta C_L(T)/C_L^0(T)$ with the temperature in all the systems except KCl:Na. These maxima are related to the appearance of quasilocal vibrations in the phonon spectrum of the host crystal due to introduction of impurities. The dips occurring in thermal conductivity curves appear to be due to the specialized modes of vibrations. In both studies the resonances appear at nearly the same frequencies in all the systems. The resonance frequencies observed by optical techniques are compared with the values obtained in the present work. The variation in force-constant changes does not affect the position of maxima in relaxation-rates-versus-frequency curves. The nature of the sodium impurity in KCl is discussed in detail. Three-phonon processes having different temperature dependences in the various temperature ranges have been used in the computations of thermal conductivity. The present theory shows reasonably good agreement with the experimental measurements on specific heat as well as with those on thermal conductivity of KCl doped with monovalent impurities.

I. INTRODUCTION

A small concentration of substitutional impurities in a crystalline lattice may give rise to exceptional (local, gap, or resonance) vibrational modes. A wide variety of experimental techniques, viz., the impurity-induced infrared absorption, Raman spectroscopy, neutron scattering, Mössbauer effect, measurement of superconducting transition temperatures, electrical resistivity, specific-heat measurements, and thermal conductivity, have been used to study the exceptional vibrational modes in ionic crystals, in polar and homopolar semiconductors and in metals. The application of several powerful methods such as optical and inelastic neutron scattering measurements are restricted to particular classes of materials and involve only particular kinds of symmetry modes, whereas the thermal conductivity and the specific-heat studies are universally applicable and involve all kinds of vibrational modes. We, therefore, present in this paper the systematic theoretical study of thermal

conductivity and specific heat of KCl doped with different monovalent point defects using the Green's-function approach.

In diatomic systems such as ionic crystals or polar semiconductors the substitutional impurities occupy sites of cubic symmetry. If the substitutional impurity atom is light enough compared to the mass of the host-lattice atom, or if it is coupled much more strongly to the neighboring atoms than the atom it replaces, one observes the localized or bound states. The frequencies of the localized states lie outside the range of the allowed phonon frequencies of the host crystal. The displacement amplitudes of the atoms in these modes decay faster than exponentially with increasing distance from the impurity site. If there exists a gap in the frequency spectrum of the crystal, the localized vibration modes appearing in the gap region are named as gap modes. There is, in fact, no fundamental distinction between a localized mode and a gap mode.

Unlike localized and gap modes, resonance

modes are not true normal modes of a perturbed harmonic crystal. If the impurity ion is very heavy and/or is coupled very weakly to the surrounding host crystal, then the behavior of its motion in low-frequency normal mode vibrations of the perturbed crystal can be viewed as follows: At very low frequencies, due to infinitesimal translation invariance, the impurity ion vibrates in phase with its neighbors in the host crystal. However, as the frequency of normal modes increases because of its large mass and/or weak binding to the crystal, it begins to lag more and more behind its neighbors, until a frequency is reached at which it begins to vibrate 180° out of phase with the surrounding lattice in a kind of local optical vibration mode. The frequency at which this occurs is called the frequency of a resonance mode. The mean-square vibration amplitude of the impurity atom as a function of its frequency is sharply peaked at the resonance mode frequency, but the mode is not spatially localized in the way that a high-frequency localized mode or gap mode is. In addition, because the frequency of a resonance mode falls in the range where the density of vibrational frequencies of the host crystal is nonzero, it can decay into the continuum of band modes and acquires a width in this manner.

The scattering of phonons due to point defects has been found in several interesting ways. As was first shown by Pomeranchuk,¹ the introduction of atoms whose mass differs from that of the host atoms leads to a phonon-scattering cross section which varies as the fourth power of the phonon frequency (Rayleigh scattering of phonons). This result was later calculated in more detail by Klemens,² who also showed that impurity atoms bound by force constants which differ from those of the host lattice also resulted in a Rayleigh-type scattering cross section. The mass-difference-only case has been well verified by earlier workers. The most complete study of the isotope effect has been described by Berman and Brock.³ The effect of the force-constant changes on the thermal conductivity still needs some more study.

The case of point defects bound by different force constants is a much more complicated one. As has been shown by many studies in alkali-halide lattices, such defects usually produce a resonant scattering of phonons. One must distinguish at least three different resonant effects. As was first shown by Pohl,⁴ defects composed of molecules have a resonant interaction with phonons. This resonant interaction has been found to

be quite complicated,^{5,6} with the molecules undergoing free rotations, librations, tunneling, etc., in the solid. In general, this resonant interaction arises from the presence of an internal structure of the molecule.

A second type of resonant behavior comes from point defects which are composed of single atoms or ions which are so small that their equilibrium site is off-center. Such defects have been studied by Pohl⁷ and co-workers. Neither the molecules nor the off-center defects will be discussed in this paper.

Our attention is on monatomic point defects of the sort discussed by Klemens in the paper described above. From the time of the paper by Walker and Pohl,⁸ with the accompanying theoretical model of Wagner,⁹ such defects have been known to perturb the lattice spectrum in a resonant manner. These resonant states have, in fact, come to be expected almost as a general rule. They manifest themselves as "dips" in the thermal-conductivity-versus-temperature plots, with the dip generally occurring near or above the peak in conductivity curve. Baumann and Pohl¹⁰ and Caldwell and Klein¹¹ have reported a broad spectrum of results in alkali halides. Harrington and Walker¹² and Chau and Klein¹³ have studied these defects in fluorite-type crystals and silver halides, respectively. On the theoretical side, the study of such lattice resonances has been a theorist's playground; a review of the theoretical work has been given by Klein.¹⁴ Recently, many other workers¹⁵⁻¹⁹ have considered the problem theoretically.

Information on such resonances can be obtained from optical properties,²⁰⁻²³ elastic properties,²⁴ and more recently from specific-heat studies.²⁵⁻²⁹ The specific heat represents the state of phonons in nonmetallic crystals and is thus an important thermal property. Introduction of crystal imperfections alters the phonon state, and thus the specific heat is changed to some extent. The measurements of the specific heat of KCl doped with monatomic impurities have been done by Karlsson²⁵ and by Kvavadze and August.^{27,28} In previous publications we have studied theoretically the specific heat of KCl:Tl⁺ (Ref. 26) and KCl:Cs⁺, I⁻ (Ref. 29) using a model that includes the effects of mass change at the impurity site and the nearest-neighbor longitudinal force-constant change. Here we have used a better lattice-dynamical model (breathing-shell model) for calculating the Green's functions, whereas previously the Green's functions

were calculated in Hardy's deformation dipole model. We have applied the theory for six impurities: TI^+ , Ag^+ , Cs^+ , Na^+ , I^- , and Br^- in KCl. The force-constant changes obtained in the case of specific heat are used to calculate the point-defect scattering in thermal conductivity. The relaxation time for the point-defect scattering due to substitutional impurities is calculated using the Green's-function method. The Green's function is configurationally averaged in the low concentration limit. The resonance frequencies computed in the study of calorimetric methods are compared with the resonance frequencies obtained for the same systems through infrared-absorption³⁰⁻³⁴ and Raman scattering results.^{35,36} In some of the systems the resonances could not be observed through optical methods, and therefore, the study of these impurity vibrations by specific-heat methods, supplemented by thermal conductivity studies is of great interest.

The structure of the paper is as follows: In Sec. II A we obtain the relaxation time in terms of self-energy for the imperfect crystal; in Sec. II B the change in specific heat in terms of phase shift is briefly discussed, and Sec. II C describes the perturbation model used in the present work. Sections III A, III B, and III C show the computation of Green's functions, specific heat, and thermal conductivity, respectively. The main conclusions are drawn in Sec. IV.

II. THEORY

A. Relaxation time for imperfect crystal

The time-independent equation of motion for a pure crystal can be written in the matrix form as

$$\underline{L}_0 \vec{\psi}_0 = \omega^2 \vec{\psi}_0, \quad (1)$$

where $\underline{L}_0 = \underline{M}_0^{-1/2} \underline{\Phi}_0 \underline{M}_0^{-1/2}$ is the mass-reduced force-constant matrix of the pure lattice and \underline{M}_0 is the mass matrix. $\vec{\psi}_0$ is a vector that is related to the usual atomic displacement \vec{u} by

$$\vec{u} = \underline{M}_0^{-1/2} \vec{\psi}_0. \quad (2)$$

\underline{L}_0 is a $3N \times 3N$ matrix for a Bravais lattice, and N is the number of nuclei in the crystal.

For a crystal containing a finite concentration of defects that have different masses and different interactions with its neighbors than the host atoms, the equation of motion may be written as

$$[\underline{L}_0 + \underline{P}(\omega^2)] \vec{\psi} = \omega^2 \vec{\psi}, \quad (3)$$

where ω is the frequency of the normal mode and $\underline{P}(\omega^2)$, the perturbation matrix caused by the defects, is explicitly given by

$$\underline{P}(\omega^2) = -\omega^2 \underline{M}_0^{-1/2} \underline{\Delta M} \underline{M}_0^{-1/2} + \underline{M}_0^{-1/2} \underline{\Delta \Phi} \underline{M}_0^{-1/2}. \quad (4)$$

Here the new mass and force-constant matrices for the imperfect crystal have been denoted by $\underline{M}_0 + \underline{\Delta M}$ and $\underline{\Phi}_0 + \underline{\Delta \Phi}$, respectively, and $\vec{\psi}$ is the corresponding vector for the imperfect lattice.

The Green's function for the perturbed crystal is defined by

$$\underline{G}(z) = [\underline{L}_0 + \underline{P}(\omega^2) - z\underline{I}]^{-1}, \quad (5)$$

with \underline{I} as a unit matrix and $z = \omega^2 + 2i\omega\eta^+$ as the complex squared frequency in the limit $\eta^+ \rightarrow 0$. It can also be expressed as

$$\underline{G}(z) = \underline{G}_0(z) - \underline{G}_0(z) \underline{P}(\omega^2) \underline{G}(z), \quad (6)$$

where the Green's function for the perfect crystal is defined by

$$\underline{G}_0(z) = (\underline{L}_0 - z\underline{I})^{-1}. \quad (7)$$

After performing a statistical average over all configurations containing the same number of defects, the configurationally averaged Green's function $\langle \underline{G} \rangle$ has the form

$$\langle \underline{G} \rangle = \underline{G}_0 - \underline{G}_0 \underline{\Sigma} \langle \underline{G} \rangle, \quad (8)$$

where the self-energy $\underline{\Sigma}$ is translationally invariant like \underline{G}_0 . After going over the normal-mode representation, the perturbed Green's function is given by

$$\langle \underline{G}(\vec{k}) \rangle = \underline{G}_0(\vec{k}) - \underline{G}_0(\vec{k}) \underline{\Sigma}(\vec{k}) \langle \underline{G}(\vec{k}) \rangle, \quad (9)$$

or

$$\langle \underline{G}(\vec{k}) \rangle = [\omega^2(\vec{k}, s) + \underline{\Sigma}(\vec{k}) - z\underline{I}]^{-1}. \quad (10)$$

Thus the real and imaginary parts of the self-energy $\underline{\Sigma}(\vec{k})$ determine the shifts and the widths of the perturbed phonons, respectively.

If we neglect the possibility of the interaction of neighboring defects, the first-order self-energy is given by³⁷

$$\underline{\Sigma}_1 = ct[\underline{I} - c\underline{G}_0 t]^{-1}, \quad (11)$$

where c is the fractional concentration of defects in the crystal. The t is the T matrix for a crystal containing one defect and is given by

$$t(z) = p(\omega^2)[\underline{I} + g(z)p(\omega^2)]^{-1}. \quad (12)$$

Here the $p(\omega^2)$ and $g(z)$ are the perturbation and

Green's-function matrices that lie in the subspace of a defect $3b \times 3b$ (b is the total number of atoms directly disturbed by the presence of a single defect including the defect site itself). For the lowest order of concentration of defects Eq. (11) may further be approximated by

$$\Sigma_1 = ct. \quad (13)$$

In order to obtain the relaxation time of lattice waves of imperfect crystal we write the above-obtained self-energy in the normal-mode representation as

$$\Sigma(\vec{k}, s) = c \sum_{s'} \langle \vec{k}, s' | t | \vec{k}, s \rangle. \quad (14)$$

In general, there is a mixing of phonon polarization branches, i.e., for a phonon of a particular polarization s , the phonons are scattered into all the polarization branches. However, in some simple cases such as that for a low concentration of defects in the mass-defect model or in the presence of force-constant changes when \vec{k} lies along certain symmetry directions, branch mixing does not occur. In cubic crystals, these symmetry directions are the well-known $(0, 0, \xi)$, $(0, \xi, \xi)$, and (ξ, ξ, ξ) directions where $\xi = k/k_{\max}$. Thus in the presence of trivial nondiagonal terms in $\Sigma(\vec{k}, s)$, we may write for one polarization branch

$$\Sigma(\vec{k}, s) = \langle \vec{k}, s | t | \vec{k}, s \rangle. \quad (15)$$

In the lowest order of concentration of defects, the inverse of the relaxation time, as limited by the defect phonon scattering, is just the imaginary part of the self-energy³⁸ with the normal-mode wave vector \vec{k} and polarization s :

$$(\tau_{\vec{k}, s}^{-1})_{\text{def}} = -c\pi\omega(\vec{k}, s)^{-1} \times \text{Im} \langle \vec{k}, s | t(z) | \vec{k}, s \rangle. \quad (16)$$

Usually the dimensions of the perturbation matrix are very large and it is difficult to evaluate the self-energy $\Sigma(k, s)$. The problem may be simplified immensely if the perturbation has some symmetry. In that case, the use of the symmetry coordinates, i.e., the coefficients of the atomic displacements of the symmetrized linear combinations of these coordinates in the impurity space, block-diagonalizes the matrices $p(\omega^2)$ and $g(z)$ simultaneously. Let $|v, m\rangle$ denote the normalized symmetry coordinate transforming according to the first row of the irreducible representation (IR) v . The index m varies from 1 to m_v , where m_v is the number of times the IR v occurs in $p(\omega^2)$. The T matrix may

then be written as

$$\begin{aligned} & \langle \vec{k}, s | t(z) | \vec{k}, s \rangle \\ &= \sum_{v, m, m'} l_v \langle \vec{k}, s | v, m \rangle t_v^{mm'}(z) \langle v, m' | \vec{k}, s \rangle, \end{aligned} \quad (17)$$

where l_v is the degeneracy of the IR v , and the contribution of one matrix element of the t matrix in the v th IR is given by

$$t_v^{mm'} = \langle v, m | t | v, m' \rangle. \quad (18)$$

B. Specific heat

The lattice specific heat of a solid per g mol is given by²⁶

$$C_L(T) = \frac{\hbar^2}{4k_B T^2} \int_0^\infty \omega^2 N(\omega) c s \hbar^2 (\hbar\omega/2k_B T) d\omega, \quad (19)$$

where $N(\omega)$ is the number of phonon states lying in the interval between ω and $\omega + d\omega$ as $d\omega \rightarrow 0$. The introduction of impurities changes the phonon density of states, and hence the lattice specific heat is also changed. If we assume that the perturbation is symmetric, the density of states can be written as the sum of the contributions from all the IR's. The change in specific heat due to impurities can thus be written as

$$\Delta C_L(T) = \sum_v \Delta C_L^v(T), \quad (20)$$

where $\Delta C_L^v(T)$ is the change in specific heat in the IR v .

The phase shifts δ_v in solid-state scattering theory is defined as

$$\tan \delta_v = -\frac{\text{Im} D_v(z)}{\text{Re} D_v(z)}. \quad (21)$$

Here $D_v(z) = |I + g_v(z)p_v(\omega^2)|$ is called the resonance denominator in the IR v . $g_v(z)$ and $p_v(\omega^2)$ are the Green's functions and perturbation matrices projected onto the subspace of IR v .

In the low concentration limit the vibrational properties can be understood only by knowing the behavior of a single impurity. One may thus determine the change in specific heat due to a single defect and multiply it by the number of defects present in the crystal.

The change in specific heat after integrating Eq. (19) once by parts and introducing the phase shifts turns out to be

$$\Delta C_L(T) = - \sum_{\nu} \frac{2k_B c N B^2}{\pi} \int_0^{\infty} \delta_{\nu} \omega \operatorname{csch}^2(B\omega) [1 - B\omega \coth(B\omega)] d\omega, \quad (22)$$

where N is the number of atoms per g mol and $B = \hbar/2k_B T$.

C. Perturbation model

We assume that the defect changes the mass at the impurity site and the nearest-neighbor central force constant with the O_h point-group symmetry. The matrix $p(\omega^2)$ is of dimension 21×21 . The IR's occurring in this problem are F_{1u} , A_{1g} , and E_g . The nearest-neighbor perturbation model for a substitutional ion in a NaCl-type lattice has been described in previous work.^{14,38,39} The expressions for the various IR of the T matrix are

$$t_{A_{1g}}(z) = \frac{1}{2} \chi \lambda \{ 1 + 2\lambda \chi [g_4^{\pm}(z) + 2g_5^{\pm}(z)] \}^{-1}, \quad (23)$$

$$t_{E_g}(z) = \frac{1}{2} \chi \lambda \{ 1 + 2\lambda \chi [g_4^{\pm}(z) - g_5^{\pm}(z)] \}^{-1}, \quad (24)$$

and

$$t_{F_{1u}}(z) = \frac{1}{D_{F_{1u}}(z)} \begin{bmatrix} \lambda + \epsilon \omega^2 & -(\chi/2)^{1/2} \lambda \\ -(\chi/2)^{1/2} & \lambda + \epsilon \omega^2 \end{bmatrix}, \quad (25)$$

where

$$D_{F_{1u}}(z) = 1 - \epsilon \omega^2 g_1^{\pm} + 2\lambda (g_1^{\pm} + \chi g_3^{\pm} - 2\chi^{1/2} g_2^{\pm}) - 2\epsilon \omega^2 \lambda \chi (g_1^{\pm} g_3^{\pm} - g_2^{\pm 2}). \quad (26)$$

Here $\chi = M_{\pm}/M_{\mp}$ denotes the host-crystal mass ratio, $\lambda = \Delta f/M_{\pm}$ denotes the change in the nearest-neighbor central force constant in units of squared frequency, and $\Delta f = f' - f_0$, where f_0 and f' represent the force constants of pure and impure crystals, respectively. The mass-change parameter ϵ is equal to $(M' - M)/M$, where M' is the mass of the impurity. The five Green's-function matrix elements are given by

$$g_{\mu}^{\pm}(z) = \frac{1}{N} \sum_{s=1}^3 \sum_{\vec{k}} \frac{J_{\mu}^{\pm}(\vec{k}|s)}{\omega_{\vec{k},s}^2 - z}, \quad (27)$$

where the summation is to be taken over all the wave vectors lying in the first Brillouin zone, and $J_{\mu}^{\pm}(\vec{k}|s)$ for $\mu = 1-5$ represents the following expressions:

$$J_1^{\pm}(\vec{k},s) = e_x^2(\pm | \vec{k},s), \quad (28a)$$

$$J_2^{\pm}(\vec{k},s) = e_x(\pm | \vec{k},s) e_x(\mp | \vec{k},s) \times \cos(2\pi r_0 k_x), \quad (28b)$$

$$J_3^{\pm}(\vec{k},s) = e_x^2(\mp | \vec{k},s) \cos^2(2\pi r_0 k_x), \quad (28c)$$

$$J_4^{\pm}(\vec{k},s) = e_x^2(\pm | \vec{k},s) \sin^2(2\pi r_0 k_x), \quad (28d)$$

and

$$J_5^{\pm}(\vec{k},s) = e_y(\mp | \vec{k},s) e_z(\mp | \vec{k},s) \times \sin(2\pi r_0 k_y) \sin(2\pi r_0 k_z). \quad (28e)$$

Here r_0 is the nearest-neighbor distance and $e_x(\pm | \vec{k},s)$ is the x th Cartesian component of the polarization vector of the lattice wave (\vec{k},s) .

The present perturbation model will give a meaningful picture of the physical situation of the defect problem if we are able to specify satisfactorily the force-constant change parameter λ . As the noncentral force-constant changes are, in general, an order of magnitude smaller than the central ones, in the alkali halides we assume λ' (noncentral force-constant change) to be equal to be zero. The presumption that the noncentral component of the force constant is much smaller than the central component, particularly in KCl, is supported by the fact that the value of the elastic constant c_{44} is not much different from that of c_{12} in KCl.⁴⁰ Also, it has been observed that the assumption $\lambda' = 0$ works well in reproducing the frequency of the low-lying resonant mode with a reasonable changed central force constant. The frequencies of a resonance mode in the IR ν are determined by

$$\operatorname{Re} D_{\nu}(z) = 0. \quad (29)$$

III. NUMERICAL COMPUTATIONS AND RESULTS

A. Green's functions

In order to calculate the complex-valued Green's functions, a detailed knowledge of the frequencies and polarization vectors of the normal modes of the pure crystal should be known. The necessary data were supplied by Dochy,⁴⁰ in which he has used the breathing-shell model of Schröder⁴¹ by taking into account the short-range forces up to second-nearest neighbors. A staggered-bin averag-

ing procedure is followed in the machine computation of the Green's functions given by Eq. (27). The Green's function is separated into real and imaginary parts as

$$g_{\mu}^{\pm}(\omega^2) = \frac{1}{N} \sum_s \sum_{\vec{k}} \frac{J_{\mu}^{\pm}(\vec{k}, s)}{\omega_{\vec{k}, s}^2 - \omega^2} + i\pi \sum_s \sum_{\vec{k}} J_{\mu}^{\pm}(\vec{k}, s) \delta(\omega_{\vec{k}, s}^2 - \omega^2). \quad (30)$$

To carry out actual integration for the real part of the Green's functions at low frequencies, the method of Sievers⁴² has been followed. We may write

$$\text{Reg}_{\mu}^{\pm}(\omega^2) = \int_0^{\omega_m} d\omega' \frac{S(\omega') - S(\omega)}{\omega'^2 - \omega^2} - \frac{S(\omega)}{2\omega} \ln \frac{\omega_m + \omega}{\omega_m - \omega}, \quad (31)$$

where

$$S(\omega) = \frac{1}{N} \sum_s \sum_{\vec{k}} J_{\mu}^{\pm}(\vec{k}, s) \delta(\omega_{\vec{k}, s} - \omega),$$

and ω_m is the maximum frequency of the lattice. The imaginary part in terms of $S(\omega)$ is given by

$$\text{Img}_{\mu}^{\pm}(\omega^2) = (\pi/2\omega) S(\omega). \quad (32)$$

The whole frequency range is divided into 60 equal bins. The value of the increment in the frequency is chosen in such a way that the spurious fluctuations appearing in the Green's functions are minimized. The value 0.5 in the units of the bin width is found to be appropriate in the present calculations.

B. Specific heat

Figures 1–4 summarize the experimental as well as theoretical results on KCl:Tl, KCl:Br, KCl:Cs(I), and KCl:Ag(Na), respectively. The influence of quasilocal oscillations (resonances) on the specific heat with heavy impurity atoms is seen most clearly in the temperature dependence of the quantity $\Delta C_L(T)/C_L^0(T)$, where $\Delta C_L(T)$ is the change in the phonon specific heats of the impure system and of the initial KCl, and $C_L^0(T)$ is the specific heat of pure KCl. For the impurity atom and its nearest perturbing neighbors, which oscillate in a relatively narrow interval of frequencies about the resonance frequency, the transition to the classical limit of the specific heat occurs at a lower

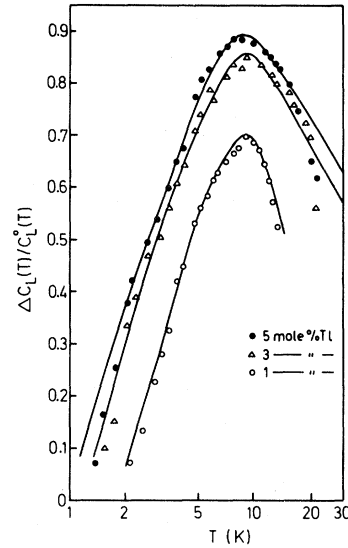


FIG. 1. Comparison between the experimental results (points) for $\Delta C_L(T)/C_L^0(T)$ and the theoretical curves (full) for KCl:Tl for $\lambda = -0.195 \times 10^{26} \text{ sec}^{-2}$.

temperature. Therefore, the quantity $\Delta C_L(T)/C_L^0(T)$ has in the presence of resonance a maximum whose position and amplitude are determined completely by the change induced in the phonon spectrum due to introduction of the heavy impurity into the crystal.

The temperature dependence of $\Delta C_L(T)/C_L^0(T)$ for the three KCl:Tl systems is shown in Fig. 1. The nature of the curve is the same for all the

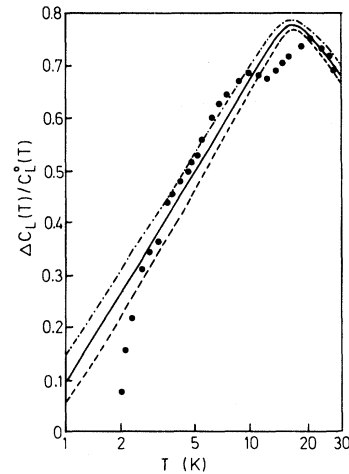


FIG. 2. Comparison between the experimental results (points) for $\Delta C_L(T)/C_L^0(T)$ and the theoretical curves for KCl:Br. — $\lambda = -0.348 \times 10^{26} \text{ sec}^{-2}$; - - - $\lambda = -0.256 \times 10^{26} \text{ sec}^{-2}$; - · - · $\lambda = -0.428 \times 10^{26} \text{ sec}^{-2}$.

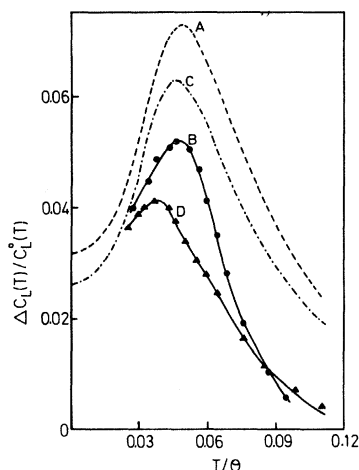


FIG. 3. Comparison between the experimental results (points) for $\Delta C_L(T)/C_L^0(T)$ and the theoretical curves for KCl containing substitutional impurities I^- , Cs^+ . Curves *A* and *C* show mass-defect calculations for I^- and Cs^+ impurities, respectively; *B* and *D* show computations for $\lambda = -0.581 \times 10^{26} \text{ sec}^{-2}$ for the I^- impurity and $\lambda = -0.475 \times 10^{26} \text{ sec}^{-2}$ for the Cs^+ impurity, respectively.

three systems. Within the limits of experimental accuracy the curves have a clearly pronounced maximum at about $T = 9 \text{ K}$. Thus the introduction of heavy Tl impurity atoms into the KCl lattice leads to the appearance of quasilocal oscillation in the phonon spectrum of impure system, a fact manifested by an appreciable deviation of the specific heat of KCl:Tl from that of KCl. The same behavior is observed in all other impurity

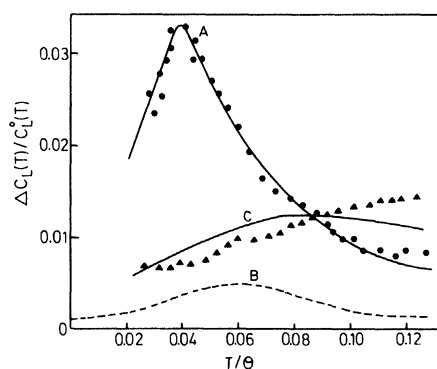


FIG. 4. Comparison between the experimental results (points) for $\Delta C_L(T)/C_L^0(T)$ and the theoretical curves for KCl containing substitutional impurities Ag^+ , Na^+ . Curves *A* and *C* show computations for $\lambda = -1.795 \times 10^{26} \text{ sec}^{-2}$ for the Ag^+ impurity and $\lambda = -1.656 \times 10^{26} \text{ sec}^{-2}$ for the Na^+ impurity, respectively. Curve *B* shows mass-defect calculations for the Ag^+ impurity.

systems except in KCl:Na, which will be discussed later.

It is natural to inquire as to what degree the observed change in the specific heat can be quantitatively described within the framework of the present theoretical concepts. In Figs. 1–4 we see the comparison of our theoretical computations with experiment with consideration of the change in mass and changes in longitudinal force constants of the interaction between the impurity and the matrix atom. A consistent theory that takes into account the change in the force constants was developed by Agrawal⁴³ and co-workers.^{22–24,26,44–46} According to their results, the deformation of the phonon spectrum of the crystal with impurity is influenced not only by the mass difference, a fact accounted for in the isotopic approximation, but also by the change in the force constants of the interaction. The weaker the heavy impurity atom is bound in the crystal, the lower the energy and sharper the distribution of quasilocal oscillation. If the force constants are very abruptly decreased, resonances can also occur for a light impurity. With this model we see a satisfactory agreement with experiment.

The impurity contribution to the specific heat has been calculated using Eq. (22) by varying the parameter λ . A number of values for λ were tried to obtain a good fit with the experimental results. A unique value of λ has been obtained to explain the experimental data successfully in every system. The obtained values of force-constant changes in the different impurity-host systems are given in Table I. The resonance frequencies from specific-heat results as well as from other defect-induced vibrational properties are also reported in this table. The frequencies calculated by us earlier in the cases of KCl:Tl and KCl:Cs(I) are shown in squared brackets. The present calculations are relatively more reliable since we have used an improved lattice-dynamical model for the calculation of Green's functions.

The behavior of KCl:Na considerably differs from that of other systems. Even at 30 K the curve does not reach its maximum value in the variation of $\Delta C_L(T)/C_L^0(T)$ versus temperature. Since sodium is a light impurity, we can assume that the effect is mainly induced by isolated impurities vibrating with relatively high frequency, as the resonance frequency at 44 cm^{-1} corresponding to vibration of $Na^+-Cl^--Na^+$ complexes^{31,32,47,48} cannot provide a continuous growth of the function up to 30 K. A detailed study by Jaswal⁴⁹ shows

TABLE I. Values of fitted force-constant changes and resonance frequencies. The values in brackets are obtained by Baumann and Pohl (Ref. 10).

Impurity	λ (10^{26} sec $^{-2}$)	Specific heat	ω_r (cm $^{-1}$) Thermal conductivity	Other results
Tl $^{+}$	-0.195	42 [41.7]	43(45)	39, ^a 51 \pm 8, ^b 125, ^c 157, ^c 74, ^d 86, ^d 122, ^d 135 ^d
Br $^{-}$	-0.348	85	85(82,86)	110 \pm 10, ^e 108.8, ^f 117.5 ^f
I $^{-}$	-0.581	56.8[56.4]	57(57)	127, ^g 198, ^h 170, ^h 69.4 ⁱ
Cs $^{+}$	-0.475	49.2[48.5]		175 ^j
Na $^{+}$	-1.656	95.5	96(77,144)	92, ^k 85.2 ⁱ
Ag $^{+}$	-1.795	53	53(53,69)	38.6, ^l 45, ^m 30 ⁿ

^aReference 59.

^bReference 25.

^cReference 35; peaks in A_{1g} symmetry in Raman scattering experiments.

^dReference 35; peaks in E_g symmetry in Raman scattering experiments.

^eReference 25.

^fReferences 50 and 60. The authors have observed strong peaks in far-infrared absorption experiments at these frequencies, but they concluded that peaks were not due to resonances.

^gReference 36; the peak in $E_g(A_{1g})$ symmetry in Raman scattering experiments. The far-infrared absorption experiments show similar behavior as that observed in the case of Br $^{-}$.

^hA. I. Stekhavov and M. B. Eliashberg, Fiz. Tverd. Tela (Leningrad) **6**, 3397 (1964) [Sov. Phys. — Solid State **6**, 2718 (1965)]; Raman scattering peak in A_{1g} and E_g symmetry.

ⁱReference 8.

^jReference 62; the peak in E_g symmetry in Raman scattering results.

^kReference 28.

^lReference 30; infrared absorption peak.

^mReference 36; strong peak in E_g symmetry in Raman scattering experiments.

ⁿReference 28.

that the far-infrared absorption is connected with the appearance of Na $^{+}$ —Cl $^{-}$ —Na $^{+}$ complexes oriented in [100] direction. He has considered the vibrations of a quasimolecule consisting of this complex and its nearest neighbors, and has found the force constant of the Na $^{+}$ —Cl $^{-}$ linkage from the condition that the minimum eigenfrequency of such a system is 44 cm $^{-1}$. Jaswal has used the so-obtained force constant for the determination of the frequency of isolated Na $^{+}$ -impurity vibrations, which appeared to be at 77.7 cm $^{-1}$. The resonance frequency associated with the isolated Na $^{+}$ impurities has not been observed by optical methods.^{33,50} We have obtained a large softening of the force constant in fitting the experimental specific-heat results and a resonant frequency at 95.3 cm $^{-1}$. This result seems to be reasonable.

The one-phonon density of states of KCl is quite large⁵¹ at 77.7 cm $^{-1}$, and the resulting impurity-

induced infrared absorption would be much more than that due to the single-defect resonance mode. It would, therefore, be difficult to observe the single-defect resonance mode experimentally. Thus, even though there is a large softening of the short-range force constant when a Na $^{+}$ ion is substituted for K $^{+}$ in KCl, the softening does not show up in the single-defect experiments because of the large impurity-induced absorption due to the one-phonon density of states of KCl.

As pointed out in the Introduction, the contribution of resonance modes to the lattice part of the specific heat is quite important. Out of the three IR's involved in the calculations, the resonances occur only in the F_{1u} irreducible representation in which the impurity atom moves. Also, in almost all the systems the maximum contribution to the specific heat comes from this IR.

Recently, Gupta and Singh⁵² have calculated the

change in specific heat due to Br^- and I^- impurities in KCl, showing good agreement with the experiment. Their calculations seem to be in error. They have shown the percentage contribution to the changed specific heats due to F_{1g} , F_{2g} , and F_{2u} modes also, whereas these modes will appear only when they consider⁵³ the effect of ΔB (in their notation). But they have neglected the effect of ΔB in their computations. Also, the shape of their curve in mass-defect calculation in the case of KCl:I^- creates doubt about the reliability of their calculations.

C. Thermal conductivity

For calculating the thermal conductivity of doped KCl we have used the expressions derived by Callaway⁵⁴:

$$K = \frac{1}{2\pi^2 v} \int_0^{\omega_D} \tau_c(\omega, T) \frac{\hbar^2 \omega^4}{k_B T^2} \frac{e^{\hbar\omega/k_B T}}{(e^{\hbar\omega/k_B T} - 1)^2} d\omega. \quad (33)$$

In this expression v is the sound velocity, ω_D is the Debye frequency, and $\tau_c(\omega, T)$ is the combined phonon relaxation time due to different scattering mechanisms. Within the framework of this model one writes the total relaxation time as a sum of reciprocal relaxation times for the separate scattering processes:

$$\tau_c^{-1}(\omega, T) = \sum_i \tau_i^{-1}(\omega, T). \quad (34)$$

There are as many τ_i as there are individual scattering mechanisms. Equation (34) is an equivalent way of stating that one adds scattering rates.

Two central approximations underlying Eq. (33) are the assumption of isotropy, in converting a conductivity tensor to a conductivity scalar, and the introduction of Debye density of states, in converting a summation over phonon states into an integral. It has been examined experimentally that there is no anisotropy in the thermal conductivity of KCl. However, there is lack of legitimacy in using an "average" sound velocity since it is known that this quantity is anisotropic. To take account of this and other issues properly one should break the conductivity integral up into a longitudinal part and a transverse part, as was done by Holland⁵⁵ and by us earlier in many cases.⁵⁶⁻⁵⁸ Such an analysis of a two-mode conduction is desirable, but this approach contains many adjustable param-

eters. Here, we are interested mainly in seeing the effect of point defects on the thermal conductivity by using a realistic model; hence we will use the approach which involves minimum number of adjustable parameters.

Equation (34) is written as

$$\tau_c^{-1}(\omega, T) = \tau_{\text{pure}}^{-1} + \tau_{\text{def}}^{-1}, \quad (35a)$$

where τ_{pure} is the relaxation time for the pure KCl and is given by

$$\tau_{\text{pure}}^{-1} = \tau_b^{-1} + \tau_{\text{iso}}^{-1} + \tau_{3\text{ph}}^{-1} \quad (35b)$$

and

$$\tau_{\text{def}}^{-1} = (\tau_{A_{1g}})^{-1} + (\tau_{E_g})^{-1} + (\tau_{F_{1u}})^{-1}. \quad (35c)$$

Here τ_b^{-1} is boundary scattering, τ_{iso}^{-1} is the relaxation time for the scattering due to natural isotopes of K and Cl in pure KCl, $\tau_{3\text{ph}}^{-1}$ is the three-phonon scattering mechanism given by

$$\tau_{3\text{ph}}^{-1} = \tau_{\mathcal{N}}^{-1} + \tau_{\mathcal{U}}^{-1}, \quad (36)$$

where \mathcal{N} denotes normal processes and \mathcal{U} denotes umklapp processes. With every relaxation time there is at least one adjustable parameter. All these constants are related in principle to fundamental constants and properties of the crystal, they are difficult to calculate and often give a poor fit to the data of the pure crystal; for this reason the constants are treated here as parameters that are not very closely related to the theoretical values. The expressions for different relaxation times are given in Table II and the values of the fitted parameters are shown in Table III.

The thermal conductivity of KCl doped with Tl^+ , Br^- , and Ag^+ was measured by Baumann and Pohl,¹⁰ and Walker and Pohl⁸ measured the thermal conductivity of KCl containing I^- and Na^+ impurities. We have no knowledge of the experimental results on the thermal conductivity of KCl doped with Cs^+ .

The numerical analysis of the measured data is done by using Eq. (33). We have used the values of the fitted force-constant changes in specific-heat studies for explaining the thermal conductivity results. Other values of the force constants were also tried for the fitting of experimental data. The computations were also performed in the mass-defect approximation only. Our results are compared with experiment in Figs. 5-9. It is observed that reasonably good agreement is found for explaining the thermal conductivity results with the force-constant changes used in specific-heat calculations.

TABLE II. Inverse relaxation times used in analyzing the thermal conductivity.
 $B_2=8B_1$, $B_3=50B_2$, and $B_4=110B_3$.

Type of scattering	Symbol	Expressions	Temperature range (K)
Boundary	τ_b^{-1}	v/L	All temperatures
Isotope, etc.	τ_{iso}^{-1}	$A\omega^4$	All temperatures
Three-phonon	τ_{3ph}^{-1}	$B_1\omega^2T^4$	$T \leq 8$
		$B_2\omega^2T^3$	$8 \leq T \leq 50$
		$B_3\omega^2T^2$	$50 \leq T \leq 110$
		$B_4\omega^2T$	$T \geq 110$

The experimental curves for KCl:Tl⁺ and Br⁻ are qualitatively similar. The dip produced by Tl⁺ ions lies at a lower temperature, and the dip caused by Br⁻ ions occurs at a relatively higher temperature. This is expected from the theory also, since Tl⁺ is greater in mass than Br⁻. However, in the case of TlCl the mass of Tl⁺ is much larger than the K⁺ ion it replaces in KCl. In addition, the lattice constant of 3.83 Å for TlCl is considerably greater than KCl, but the lattice constant of KBr is not greatly different from that of KCl. This shows that in the case of KCl:Tl⁺ the contribution due to mass defects dominates over the contribution due to force-constant changes. We have seen that the impurity contributions to the specific heat due to the force constant in this system is small as was also observed earlier,²⁶ whereas in the case of KCl:Br⁻ the contribution due to force-constant changes is comparatively larger.

In Fig. 10 we plotted the relaxation rates for thallium impurity ($3.6 \times 10^{18} \text{ cm}^{-3}$) for $\lambda = -0.195 \times 10^{26} \text{ sec}^{-2}$. The contributions due to different IR's are also shown separately. If we change the value of λ we see a small effect on the height and width of the peak of $1/\tau_d$, but its position does not shift appreciably from 43 cm^{-1} , which is the value of the resonance frequency in

TABLE III. Values of parameters used in the analysis of thermal conductivity.

Θ	230 K ^a
v	$2.45 \times 10^5 \text{ cm sec}^{-1}$
L	0.41 cm
A	$8.7 \times 10^{-44} \text{ sec}^3$
B_1	$4.8 \times 10^{-24} \text{ sec deg}^{-3}$

^aReference 10.

F_{1u} symmetry modes. Baumann and Pohl¹⁰ obtained the resonance frequency at 45 cm^{-1} using an empirical relation between frequency and temperature [Eq. (2) of their paper]. However, as they have discussed, the accuracy of the empirical relation is within 20%; therefore, the value of the resonance frequency obtained by us is quite reasonable. We get a sharp peak at the resonance frequency if we plot a graph between reduced relaxation rate (τ_d^{-1}/ω^4) and frequency. Other experimental information about the resonance frequency is given by Kahan and Sievers,⁵⁹ who got a weak line in infrared absorption measurements at about 39 cm^{-1} . Our specific-heat results give the same resonance frequency as obtained in thermal conductivity calculations.

The impurity bromine is roughly twice as heavy as the host ion for which it is substituted. Figure 11 shows the plot of the reduced relaxation rates for the lowest concentration of bromine ($4 \times 10^{19} \text{ cm}^{-3}$) and for two values of λ . From the figure

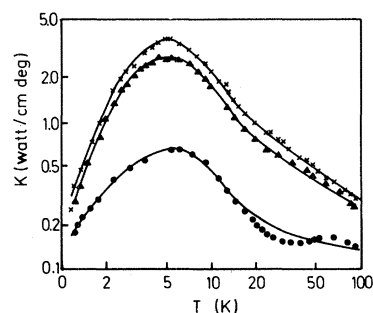


FIG. 5. Thermal conductivity of KCl:Tl. Solid curves show present calculations for $\lambda = -0.195 \times 10^{26} \text{ sec}^{-2}$ and points are experimental results for the Tl⁺ concentrations as ($\times \times \times$), $3.6 \times 10^{18} \text{ cm}^{-3}$; ($\triangle \triangle \triangle$), $7 \times 10^{18} \text{ cm}^{-3}$; ($\bullet \bullet \bullet$), $8.6 \times 10^{19} \text{ cm}^{-3}$.

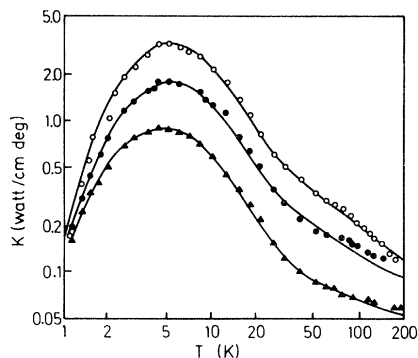


FIG. 6. Thermal conductivity of KCl:Br. Solid curves show present calculations for $\lambda = -0.348 \times 10^{26} \text{ sec}^{-2}$ and points are experimental results for Br^- concentrations as $\circ\circ\circ$, $4 \times 10^{19} \text{ cm}^{-3}$; $\bullet\bullet\bullet$, $1.6 \times 10^{20} \text{ cm}^{-3}$; $\triangle\triangle\triangle$, $8.08 \times 10^{20} \text{ cm}^{-3}$.

we see that there is a small effect on the curve due to force-constant changes, but the position of the peak is not shifted appreciably from 85 cm^{-1} . The entire curve is higher than that for thallium. In this system we also see the major contribution of odd configuration vibrational modes. Impurity-induced far-infrared absorption was measured by Weber and Siebert⁶⁰ and by Ward and Timusk.⁵⁰ These authors detected a strong peak at 108.8 cm^{-1} and a weak peak at 117.5 cm^{-1} . They concluded, however, that this peak is not caused by a resonant mode but rather by a maximum in the density of states of the host at this frequency (108.8 cm^{-1}), whereas Karo and Hardy⁵¹ observed large density of states at 77.7 cm^{-1} . Recent Raman scattering measurements⁶¹ on KCl and KBr mixed crystals have revealed no structure below 120

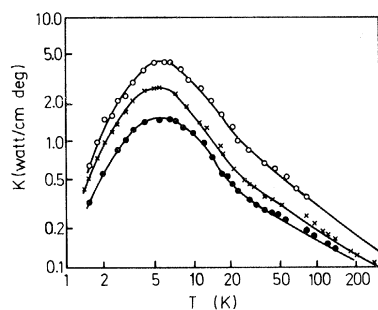


FIG. 7. Thermal conductivity of KCl:I. Solid curves show present calculations for $\lambda = -0.581 \times 10^{26} \text{ sec}^{-2}$ and points are experimental results for Br^- concentrations: $\circ\circ\circ$, $1.0 \times 10^{18} \text{ cm}^{-3}$; $\times\times\times$, $1.25 \times 10^{19} \text{ cm}^{-3}$; $\bullet\bullet\bullet$, $5.0 \times 10^{19} \text{ cm}^{-3}$.

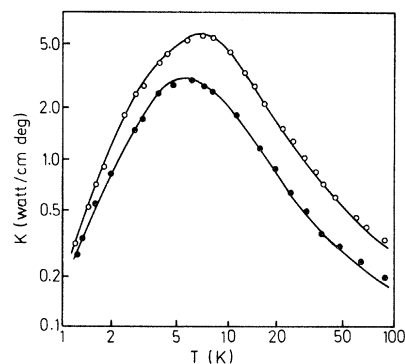


FIG. 8. Thermal conductivity of KCl:Na. Solid curves are present calculations for $\lambda = -1.656 \times 10^{26} \text{ sec}^{-2}$ and points are experimental results for Na^+ concentrations: $\bullet\bullet\bullet$, $2.3 \times 10^{19} \text{ cm}^{-3}$; $\circ\circ\circ$, pure KCl for $\lambda = 0$.

cm^{-1} . Our results on specific heat give only changes in the density of states, so we cannot explain these results in the same way as Weber and Siebert and Ward and Timusk have done. We believe that the dip in the thermal conductivity as well as the enhancement in specific heat in KCl:Br^{-1} is due to lattice resonance modes.

In the case of KCl:I^- the dip in thermal conductivity is not so pronounced as that for TI^+ and Br^- impurities. However, as the concentration of impurities increases we see a dip⁸ around 25 K . We expect similar results in the KCl:Cs^+ system. The masses of I^- and Cs^+ are approximately 4 times as heavy as the ions they substitute in KCl. The scattering rate at low frequencies is about 4 times as strong as that for bromine, and the peak is

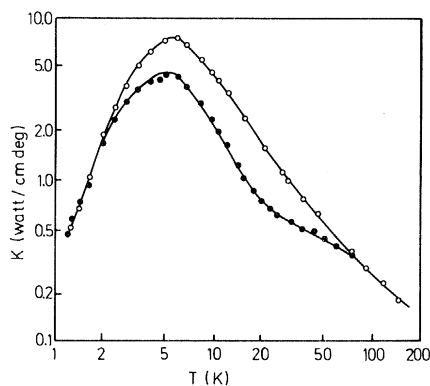


FIG. 9. Thermal conductivity of KCl:Ag. Solid curves are present calculations for $\lambda = -1.795 \times 10^{26} \text{ sec}^{-2}$ and points are experimental results for Ag^+ concentrations: $\bullet\bullet\bullet$, $1.0 \times 10^{19} \text{ cm}^{-3}$; $\circ\circ\circ$, pure KCl for $\lambda = 0$.

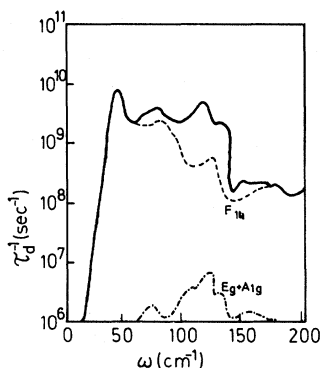


FIG. 10. Relaxation rates for TI^+ impurity ($3.6 \times 10^{18} \text{ cm}^{-3}$) in KCl for $\lambda = -0.195 \times 10^{26} \text{ sec}^{-2}$. Solid curve shows total contributions from all the three symmetry modes. Contributions from F_{1u} and $E_g + A_{1g}$ are shown separately.

also about 4 times as strong as that for bromine. We have obtained a resonance at $\omega_r = 57 \text{ cm}^{-1}$ in F_{1u} symmetry modes in case of KCl:I^- . The far-infrared absorption experiments⁵⁰ on KCl:I^- give similar results, as was observed in case of KCl:Br^- . The only difference is that the peak at 108 cm^{-1} is broader in this case. The Raman scattering experiments³⁶ on KCl:I^- show peaks in A_{1g} and E_g modes at the high-frequency part of the phonon spectrum. We observe that the contribution to the specific heat is comparatively larger due to even parity modes in KCl:I^- , Cs^+ as compared to other defect systems studied here. The contribution to the total relaxation rates due to A_{1g} and E_g modes have similar behavior. Recently, impurity-induced Raman scattering spectra of Cs^+

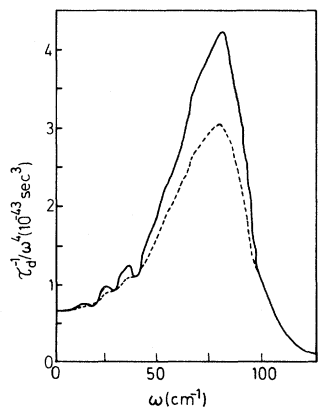


FIG. 11. Reduced relaxation rates for Br^- impurity ($4.0 \times 10^{19} \text{ cm}^{-3}$, in KCl for $\lambda = -0.348 \times 10^{26} \text{ sec}^{-2}$ (solid curve) and $\lambda = -0.285 \times 10^{26} \text{ sec}^{-2}$ (dashed curve).

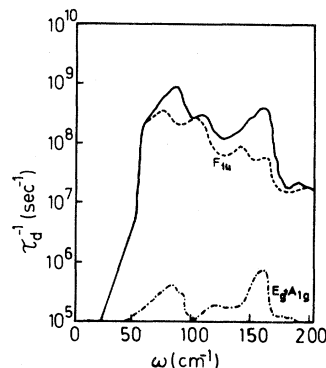


FIG. 12. Relaxation rates for Na^+ impurity in KCl for $\lambda = -1.656 \times 10^{26} \text{ sec}^{-2}$. Solid curve represents total contribution from all three symmetry modes. Separate contributions from F_{1u} and $E_g + A_{1g}$ are also shown.

in KCl have also been measured.⁶² A peak in E_g symmetry modes is observed at 175 cm^{-1} , and there is no peak above 200 cm^{-1} as observed by Stekhanov and Maksimova.⁶³

The system KCl:Na shows a slight change in the slope of the conductivity curve at about 30 K, even though the concentration of the impurity is as high as $2.3 \times 10^{19} \text{ cm}^{-3}$. The total theoretical relaxation rates for $\lambda = 1.656 \times 10^{26} \text{ sec}^{-2}$ have been shown in Fig. 12. The plot of the reduced relaxation rates for this value of λ along with $\lambda = -1.984 \times 10^{26} \text{ sec}^{-2}$ appears in Fig. 13. The structure in these curves is small and will make only a token contribution to the resistivity. We have observed a resonance at $\omega_r = 96 \text{ cm}^{-1}$ at the high-frequency side. The detailed behavior of the sodium impurity has already been discussed in Sec. III B.

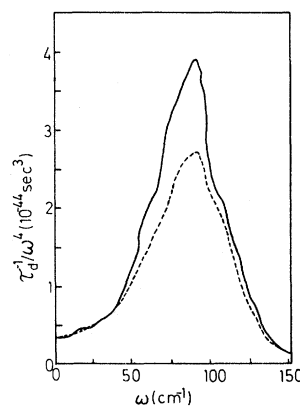


FIG. 13. Reduced relaxation rates for Na^+ impurity in KCl for $\lambda = -1.656 \times 10^{26} \text{ sec}^{-2}$ (solid curve) and $\lambda = -1.984 \times 10^{26} \text{ sec}^{-2}$ (dashed curve).

The silver impurity in KCl shows a well-pronounced dip in the thermal conductivity curve above 20 K. This impurity, despite the facts that it has a larger mass than potassium and that the compressibility of AgCl is smaller than that of KCl, has also a large negative change in the force constant when placed in KCl. In fitting the data we observe about 70% softening in the force constant of this system. This result agrees to that determined from far-infrared absorption experiments.⁶⁴ However, the infrared results give a resonance at 38.6 cm^{-1} , whereas we get a resonance at 53 cm^{-1} in both the calorimetric studies. First-order impurity-induced Raman scattering experiments³⁶ show very strong peaks in the E_g IR and negligible contributions to the spectra due to A_{1g} modes. In Fig. 14 we plot the contribution to the total relaxation rates from different IR's. As shown in the figure, F_{1u} modes have a dominating effect on the resonance scattering, and E_g and A_{1g} modes make a small contribution.

Recently, Almukhov and Zavt¹⁹ have calculated the thermal conductivity of KCl containing monovalent impurities (Tl^+ , I^- , Ag^+ , and F center) by using another approach based on the general theory of irreversible processes⁶⁵ in which the thermal conductivity is related to the correlation function of the heat fluxes. The Green's function was averaged over a random distribution of impurity atoms. The results of Almukhov and Zavt differed considerably from experiment. For the discrepancies, they have suggested additional anharmonic processes for KCl:Ag^+ , I^- , and F center, whereas for the KCl:Tl^+ system they have suggested a

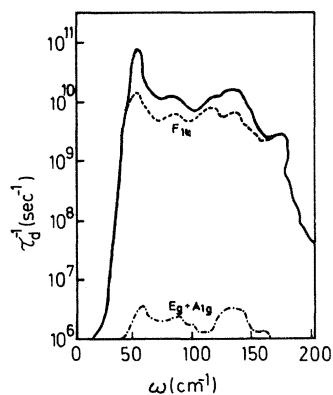


FIG. 14. Relaxation rates for Ag^+ impurity in KCl for $\lambda = -1.795 \times 10^{26} \text{ sec}^{-2}$. Solid curve shows total contribution from all three symmetry modes. Contributions from F_{1u} and $E_g + A_{1g}$ are shown separately.

correction proportional to c^2 . It is desirable to have similar modifications for all the systems.

Our calculated results are in good agreement with experiment. Besides the point-defect scattering discussed above we have also considered different temperature dependences of three-phonon relaxation times in different temperature ranges. There were many suggestions in the past for the temperature dependences of three-phonon processes, but the suggestion of Guthrie⁶⁶ is widely used in many systems. He suggested that three-phonon relaxation times can be expressed as T^{-m} , where m is an exponent which is a function of temperature. Since then, many workers^{56-58,67-69} have used this suggestion successfully in explaining the thermal conductivity of different systems. In the present case we have taken $\tau_{3\text{ph}}^{-1} = B_1 \omega^2 T^m$ for both normal and umklapp three-phonon processes. The temperature dependences in different temperature ranges are shown in Table II.

IV. CONCLUSIONS

The temperature dependence of the specific heat and thermal conductivity of KCl doped with monovalent impurities can be well understood on the basis of a localized perturbation model in which consideration of mass change at the impurity site as well as changes in the nearest-neighbor longitudinal force constant is taken into account. In the case of Ag^+ we have observed a softening of the force constant of over 70%, and light substitutional Na^+ impurities are ascribed to the vibration of isolated ions with the force constant weakened to 60%. The thallium impurity behaves as does an "isotopic" defect. Depressions of the thermal conductivity curve are almost at the same positions as those found experimentally. As was suggested by Guthrie⁶⁷ and Caldwell and Klein¹¹ (for better relaxation rates for three-phonon processes), we have used different relaxation rates in different temperature ranges for three-phonon processes. We have compared the calorimetric results with the available optical measurements. In the cases of the KCl:Br^- , I^- systems, resonance frequencies have not been observed in infrared absorption experiments, whereas a strong peak has been seen at 108 cm^{-1} (Van Hove frequency) in both systems. In the case of Na^+ a pair-vibration-induced line has been observed in far-infrared absorption experiments and resonance connected with isolated impurities has not been seen. The KCl:Ag^+ system gives resonant frequency in

far-infrared measurements as well as in calorimetric methods. A weak line has been observed in infrared absorption experiments in the case of Tl^+ impurities. Thus, resonances not detected for isolated impurities Br^- , I^- , Na^+ in KCl by means of the infrared spectroscopy has been revealed by calorimetric methods. The resonance for Cs^+ impurities has been predicted through specific-heat studies for future optical experiments. We have seen in a number of papers^{26,29,44-46} that the present model holds well for specific-heat studies. Here we have seen that the parameters found in specific-heat results explain other defect-induced vibrational properties, as was observed earlier in cases of metals.^{45,46}

ACKNOWLEDGMENTS

The author is grateful to Dr. F. Dochy, Gent, for sending the necessary data for calculating the Green's functions. Dr. Bal K. Agrawal, Professor G. S. Verma, Professor B. S. Rajput, and Professor H. H. Mende are thanked for their interest in the present work. Computational help by Dr. G. Thummes is greatly appreciated. The author is also grateful to the Alexander von Humboldt Foundation, Bonn, for awarding a fellowship, and to Garhwal University for granting a leave of absence.

*Permanent address: Department of Physics, Garhwal University, Srinagar-246 174, Garhwal, India.

¹I. Pomeranchuk, J. Phys. (USSR) **6**, 237 (1942).

²P. G. Klemens, Proc. Phys. Soc. London Ser. **A68**, 1113 (1965); Solid State Physics **7**, 1 (1958).

³R. Berman and J. C. F. Brock, Proc. R. Soc. London Ser. **A 289**, 46 (1965).

⁴R. O. Pohl, Phys. Rev. Lett. **8**, 481 (1962).

⁵B. Wedding and M. V. Klein, Phys. Rev. **177**, 1274 (1969).

⁶V. Narayanmurthy and R. O. Pohl, Rev. Mod. Phys. **42**, 201 (1970).

⁷R. O. Pohl, V. L. Taylor, and W. M. Goubau, Phys. Rev. **178**, 1431 (1969); N. E. Byer and H. S. Sack, J. Phys. Chem. Solids **29**, 677 (1968).

⁸C. T. Walker, and R. O. Pohl, Phys. Rev. **131**, 1433 (1963).

⁹M. C. Wagner, Phys. Rev. **131**, 1443 (1963).

¹⁰F. C. Baumann and R. O. Pohl, Phys. Rev. **163**, 843 (1967).

¹¹R. F. Caldwell and M. V. Klein, Phys. Rev. **158**, 851 (1967).

¹²J. A. Harrington and C. T. Walker, Phys. Rev. **B 1**, 882 (1970).

¹³C. K. Chau and M. V. Klein, Phys. Rev. **B 1**, 2642 (1970).

¹⁴M. V. Klein, in *Physics of Color Centers*, edited by W. B. Fowler (Academic, New York, 1968).

¹⁵Bal K. Agrawal, J. Phys. **C 2**, 252 (1969).

¹⁶M. D. Tiwari, Phys. Lett. **32A**, 213 (1970).

¹⁷Bal K. Agrawal, J. Phys. **C 3**, 1002 (1970).

¹⁸K. Ohashi and M. Awano, J. Phys. Soc. Japan **37**, 840 (1974).

¹⁹V. I. Almukhov and G. S. Zavt, Fiz. Tverd. Tela (Leningrad) **13**, 2438 (1971) [Sov. Phys. — Solid State **13**, 2041 (1972)].

²⁰A. J. Sievers, in *Localized Excitations in Solids*, edited

by R. F. Wallis (Plenum, New York, 1968).

²¹A. S. Barker, Jr. and A. J. Sievers, Rev. Mod. Phys. **47**, Suppl. 2, S1 (1975).

²²P. N. Ram and M. D. Tiwari, Phys. Status Solidi **B 94**, 721 (1979); P. N. Ram and Bal K. Agrawal, *ibid.* **61**, 341 (1974).

²³P. N. Ram and Bal. K. Agrawal, Phys. Status Solidi **B 55**, 729 (1973).

²⁴K. M. Kesharwani and Bal K. Agrawal, Phys. Rev. **B 5**, 2130 (1972); **4**, 4623 (1971); **8**, 3056 (1973).

²⁵A. V. Karlsson, Phys. Rev. **B 2**, 3332 (1970).

²⁶M. D. Tiwari and Bal K. Agrawal, Phys. Rev. **B 7**, 4665 (1973).

²⁷K. A. Kvavadze and G. R. Augst, Fiz. Tverd. Tela (Leningrad) **16**, 1772 (1974) [Sov. Phys. — Solid State **16**, 1149 (1974)].

²⁸G. R. Augst and K. A. Kvavadze, Phys. Status Solidi **B 72**, 103 (1975).

²⁹M. D. Tiwari, P. N. Ram, and V. K. Manchanda, J. Phys. (Paris) Colloq. Suppl. **7**, C6-272 (1980).

³⁰A. J. Sievers, Phys. Rev. Lett. **13**, 310 (1964).

³¹T. L. Templeton and B. P. Clayman, Solid State Commun. **9**, 697 (1971).

³²T. L. Templeton and B. P. Clayman, Phys. Rev. **B 6**, 4004 (1972).

³³R. W. Ward and T. Timusk, Phys. Rev. **B 5**, 2351 (1972).

³⁴A. M. Kahan and A. J. Sievers (private communication in Ref. 25).

³⁵R. T. Harley, J. B. Page, and C. T. Walker, Phys. Rev. **B 3**, 1365 (1971).

³⁶W. Möller, and R. Kaiser, Phys. Status Solidi **B 50**, 155 (1972).

³⁷R. J. Elliott and D. W. Taylor, Proc. R. Soc. London **296A**, 161 (1967).

³⁸M. V. Klein, Phys. Rev. **141**, A716 (1966).

³⁹G. Benedek and G. F. Nardelli, J. Chem. Phys. **48**,

- 5242 (1968); Natl. Bur. Std. (US) Publ. 287, 161 (1967).
- ⁴⁰F. Dochy, Phys. Status Solidi A 59, 531 (1980).
- ⁴¹U. Schröder, Solid State Commun. 4, 347 (1966).
- ⁴²A. J. Sievers, A. A. Maradudin, and S. S. Jaswal, Phys. Rev. 138, A272 (1965).
- ⁴³Bal K. Agrawal, Phys. Rev. 186, 712 (1969); J. Phys. C 2, 252 (1969).
- ⁴⁴M. D. Tiwari, Phys. Status Solidi B 98, 559 (1980); 104, 2, 751 (1981); Phys. Rev. B 24, 4502 (1981).
- ⁴⁵M. D. Tiwari and Bal K. Agrawal, Phys. Rev. B 8, 1397 (1973).
- ⁴⁶B. D. Indu, M. D. Tiwari, and Bal K. Agrawal, J. Phys. F 8, 755 (1978).
- ⁴⁷T. L. Templeton and B. P. Clayman, Bull. Am. Phys. Soc. 17, 619 (1972).
- ⁴⁸W. Moeller, R. Kaiser, and H. Bilz, Phys. Lett. 32A, 171 (1970).
- ⁴⁹S. S. Jaswal, Phys. Lett. 42A, 309 (1972).
- ⁵⁰R. W. Ward and T. Timusk, Phys. Rev. Lett. 22, 396 (1969).
- ⁵¹A. M. Karo and J. R. Hardy, Phys. Rev. 129, 2024 (1963).
- ⁵²R. K. Gupta and A. K. Singh, Solid State Commun. 29, 607 (1979).
- ⁵³R. K. Gupta and A. K. Singh, Phys. Status Solidi B 91, 697 (1979).
- ⁵⁴J. Callaway, Phys. Rev. 113, 1046 (1959).
- ⁵⁵M. G. Holland, Phys. Rev. 132, 2461 (1963).
- ⁵⁶M. D. Tiwari and Bal K. Agrawal, Phys. Rev. B 4, 3527 (1971).
- ⁵⁷Y. P. Joshi, M. D. Tiwari, and G. S. Verma, Phys. Rev. B 1, 642 (1970).
- ⁵⁸M. D. Tiwari, in Physics of Semiconductors, edited by F. G. Fumi (Topographia, Rome, 1976), p. 220.
- ⁵⁹A. M. Kahan and A. J. Sievers (Ref. 25, p. 3336).
- ⁶⁰R. Weber and F. Siebert, Z. Phys. 213, 273 (1968).
- ⁶¹I. Nair and C. T. Walker, Phys. Rev. B 3, 3446 (1971).
- ⁶²J. H. Zu Siederdisen, Phys. Status Solidi B 73, 239 (1976).
- ⁶³A. I. Stekhanov and T. I. Maksimova, Fiz Tverd. Tela (Leningrad) 8, 924 (1966) [Sov. Phys. — Solid State 8, 737 (1966)].
- ⁶⁴A. J. Sievers, in *Elementary Excitations in Solids* (Plenum, New York, 1968), p. 193; Ref. 30.
- ⁶⁵R. Kubo, M. Yokota, and S. Nakajima, J. Phys. Soc. Jpn. 12, 203 (1957); J. McLennan, Phys. Rev. 115, 1405 (1959); L. M. Luttinger, *ibid.* 135, 1505 (1964).
- ⁶⁶G. L. Guthrie, Phys. Rev. 152, 801 (1966).
- ⁶⁷G. Le Guillou and H. J. Albany, Phys. Rev. B 5, 2301 (1972).
- ⁶⁸D. N. Talwar, B. K. Ghosh, and Bal K. Agrawal, Phys. Rev. B 18, 1762 (1978).
- ⁶⁹P. C. Sharma, K. S. Dubey, and G. S. Verma, Phys. Rev. B 3, 1985 (1971).